Crack length correction and root rotation angle in a sandwich single cantilever beam (SCB) fracture specimen

Saseendran, Vishnu; Carlsson, Leif A.; Berggreen, Christian; Seneviratne, Waruna

Published in:
International Journal of Lightweight Materials and Manufacture

Link to article, DOI:
10.1016/j.ijlmm.2020.06.005

Publication date:
2020

Document Version
Publisher's PDF, also known as Version of record

International Journal of Lightweight Materials and Manufacture 3 (2020) 426–434

Contents lists available at ScienceDirect

International Journal of Lightweight Materials and Manufacture

journal homepage: https://www.sciencedirect.com/journal/international-journal-of-lightweight-materials-and-manufacture

Original Article

Crack length correction and root rotation angle in a sandwich single cantilever beam (SCB) fracture specimen

Vishnu Saseendran [a,*], Leif A. Carlsson [b], Christian Berggreen [c], Waruna Seneviratne [a]

[a] National Institute for Aviation Research (NIAR), Wichita State University, 1845 Fairmount Street, Wichita, KS, 67260, USA
[b] Department of Ocean & Mechanical Engineering, Florida Atlantic University, 777 Glades Road, Boca Raton, FL, 33431, USA
[c] Department of Mechanical Engineering, Technical University of Denmark, Nils Koppels Allé, Kgs. Lyngby, 2800, Denmark

ARTICLE INFO

Article history:
Received 20 February 2020
Received in revised form
12 June 2020
Accepted 16 June 2020
Available online 4 July 2020

Keywords:
Sandwich
Composites
Root rotation
Face sheet/core interface
Phase angle
MBT

ABSTRACT

Crack root rotation is a measure of deviation from clamped boundary conditions of region in front of the crack tip. The root rotation depends on the shear force and bending moment acting at the crack tip. Such rotation significantly affects the compliance and energy-release rate. Crack root rotation analysis of Single Cantilever Beam (SCB) sandwich specimens is presented here. Closed-form solutions for the root rotation angle obtained from the foundation analysis are compared to finite element analysis (FEA) predictions. The derived expressions closely match for a range of sandwich configurations. An expression for the energy-release rate, derived from the foundation analysis was found to agree with FEA predictions over a large range of face-to-core modulus ratios. Energy-release rate and mode mixity phase angle increased with decreasing crack length due to the transverse shear effects. At longer crack lengths, both energy-release rate and phase angle reached a value independent of crack length. The foundation model is used to derive a simple expression for the offset crack length for the SCB sandwich fracture test. It is shown that the obtained formulation agrees closely well with both numerical and experimental values. In addition, SCB fracture tests performed using an in-house built translatable rig showed close relation to both analytical and numerical compliance results.

1. Introduction

The Single Cantilever Beam (SCB) sandwich fracture specimen [1,2] is a test method to determine the face/core debond toughness of sandwich panels. The SCB test has recently been proposed to become an ASTM international testing standard [3] to perform fracture characterization of sandwich specimens under predominant mode I conditions. The sandwich SCB specimen contains a face/core interface crack at the edge of the test specimen, see Fig. 1. The lower face sheet is firmly held to the base. A loading rod attached to a loading block or hinge allows application of vertical load similar to a peel loading scenario. A schematic illustration of sandwich SCB specimen is shown in Fig. 1. At a critical load, the crack propagates a certain length, which is recorded using a suitable device. The load and displacement record is used to calculate critical energy-release rate, usually referred to as interface fracture toughness using a suitable data reduction technique [4]. It is widely recognized that the region in front of the crack tip deforms as a result of the shear force and bending moment acting on the cross-section at the crack tip [5–7]. Such deformation is measured by the rotation angle, ϕ, of the face sheet and has been termed "crack root rotation" by Li et al. [8]. The impact of root rotation, ϕ, on the crack loading and fracture parameters was studied by Li et al. [8] and Andrews and Massab [9].

Crack root rotation, which is a general effect, is not an independent contributor to the energy-release rate. However, root rotation plays a vital role in the fracture mechanics properties of beam-like geometries if there is a significant change in geometry [8]. The SCB loading investigated here contains moment and shear components. The energy-release rate is calculated using the moment and force which act at the clamped boundary of top face sheet (see Fig. 1). In case of sandwich SCB specimens, the assumption of clamped boundary condition (zero root rotation) is often violated by thin-compliant face sheets. This causes significant

* Corresponding author.
E-mail address: vsaseendran@niar.wichita.edu (V. Saseendran).
Peer review under responsibility of Editorial Board of International Journal of Lightweight Materials and Manufacture

https://doi.org/10.1016/j.ijlmm.2020.06.005

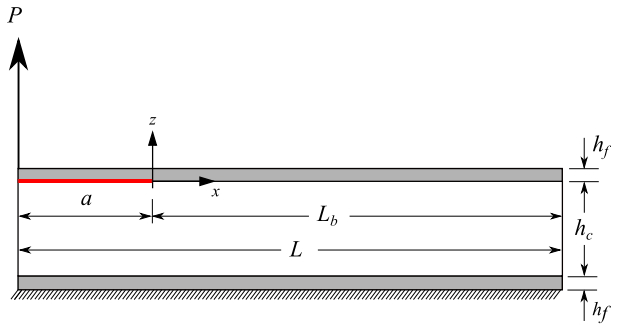

Fig. 1. Schematic illustration of SCB sandwich specimen with face sheets of thickness, h_f, and a core of thickness, h_c.

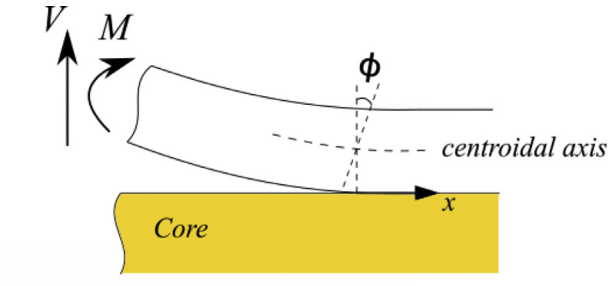

Fig. 2. Crack root rotation angle, ϕ.

errors in calculation of crack tip moment and force components. Hence, the effect of root rotation must be incorporated for accurate moment and force calculations, which is primarily governed by face and core mechanical and geometrical properties. A foundation model analysis of the root rotation angle in both force- and moment-loaded SCB sandwich specimens was presented by Saseendran et al. [10]. Recently, Kardomateas et al. [11] utilized the elasticity and a higher-order sandwich panel theory to obtain elastic constants in foundation models.

The primary objective of this paper is to examine the effect of face and core moduli and thicknesses on crack root rotation in a SCB sandwich specimen, and normalization of the results. In addition, fracture mechanics parameters such as the energy-release rate, G, and mode mixity phase angle, ψ, will be examined. The interface fracture toughness, G_c is commonly evaluated based on the compliance, C, according to the modified beam theory (MBT) method [3]. This approach requires an offset crack length that quantifies the difference in crack length due to root rotation. We will examine the relation between the offset crack length, and foundation parameters. The closed-form expression for offset crack length and compliance are compared against SCB fracture tests. Typical aerospace grade CFRP/honeycomb core sandwich specimens were employed.

2. Analysis

2.1. Analysis of crack root rotation angle, ϕ

An expression for the root rotation angle, ϕ, in the following dimensionless form has been suggested by Li et al. [8],

$$\phi = c_V \frac{V}{\bar{E}_f h_f} + c_M \frac{M}{\bar{E}_f h_f^2} \tag{1}$$

in which $\bar{E}_f$ and $\bar{E}_c$ are the face sheet and core elastic moduli; $\bar{E} = E$, and $\bar{E} = E/(1-\nu^2)$ for plane stress and plane strain, respectively, and ν is the Poisson's ratio. Coefficients c_M and c_V depend on face sheet and core stiffnesses. M is the moment and V is the shear force in the upper face sheet (per unit width). A primary objective of this analysis is to establish the parameters c_V and c_M for the SCB sandwich specimen. The analysis is based on the foundation model of the SCB sandwich specimen (Fig. 1), where the face sheet in front of the crack tip is resting on a soft core. This configuration has been perceived as a beam being supported by a Winkler foundation [5,7,10]. From our previous foundation model analysis [10], the root rotation angle, ϕ (Fig. 2), for a force-loaded SCB sandwich specimen can be expressed in terms of foundation modulus, k, as:

$$\phi = \frac{2\lambda^2 P}{k} + \frac{4a\lambda^3 P}{k} \tag{2}$$

where P is the load applied, a is the crack length (Fig. 1), and

$$\lambda = \sqrt[4]{\frac{k}{4\bar{E}_f I_f}} \tag{3a}$$

$$k = \frac{\bar{E}_c b}{h_c/4} \tag{3b}$$

where $I_f = bh_f^3/12$ with b being the specimen width.

Substituting Equation (3) in (2) yields:

$$\phi = \left(\frac{P}{b}\right)\frac{\lambda^2 h_c}{2\bar{E}_c} + \left(\frac{P}{b}\right)\frac{a\lambda^3 h_c}{\bar{E}_c} \tag{4}$$

By comparing the terms in Equations (4) and (1), and with $V = P/b$; $M = Pa/b$, the coefficients can be re-expressed as:

$$\frac{c_V}{\bar{E}_f h_f} = \frac{h_c \lambda^2}{2\bar{E}_c} \tag{5a}$$

$$\frac{c_M}{\bar{E}_f h_f^2} = \frac{h_c \lambda^3}{\bar{E}_c} \tag{5b}$$

Substitution of λ given in Equation (3a) in (5) leads to:

$$c_V = \sqrt{\frac{3h_c \bar{E}_f}{h_f \bar{E}_c}} \tag{6a}$$

$$c_M = 12^{(3/4)} \sqrt[4]{\frac{h_c \bar{E}_f}{h_f \bar{E}_c}} \tag{6b}$$

2.2. Finite element (FE) analysis

A parametric finite element study was performed to examine the root rotations in SCB specimens. A 2D FE model was constructed using ANSYS® [12]. Schematic illustration of the model is shown in Fig. 3. Linear Plane 182 element-type was used around the crack tip

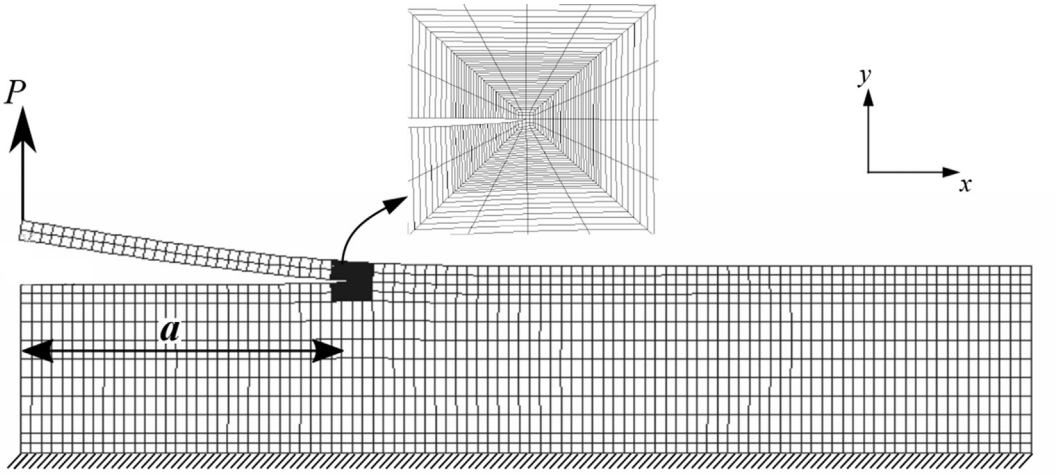

Fig. 3. Finite element (FE) model of SCB sandwich specimen.

along a ring of four elements. The minimum element edge length was 2.5 μm. The linear elements accommodate excessive deformations encountered in the near tip region. Rest of the model comprised of parabolic Plane 183 element type. The FE-model was also utilized to calculate energy-release rate, G, and phase angle, ϕ, based on the crack surface extrapolation (CSDE) method [13]. The CSDE method, briefly outlined in Appendix A, utilizes relative crack opening and sliding displacements behind the crack tip to calculate both G and ψ. The phase angle, ψ, is a measure of the mode II component of the stress intensity factor [14]. In the reduced formulation (Appendix A), $\psi = 0^{\circ}$ corresponds to pure mode I loading. It should be noted that the numerical energy-release rate presented here using the formulation presented by Hutchinson and Suo [14] does not include the damage zone. In order to model the damage zone ahead of the crack tip, cohesive zone modeling should be utilized and is out of scope of this work. Hence, the current analysis is valid within the ambit of linear elastic fracture mechanics, wherein the specimens do not develop large damage zones ahead of the crack tip. A crack propagation study employing cohesive layer at the face sheet/core interface for typical honeycomb core SCB sandwich specimens was presented in Ref. [15].

Analyses were performed to study the influence of material and geometrical parameters of the face sheet and core on the rotation angle, ϕ, compliance and the fracture parameters of the SCB specimen. In particular, thickness and modulus of both core and face sheet were varied. Sandwich specimens with aluminum and E-glass/epoxy face sheets, and various PVC foam core and one aluminum honeycomb core were considered. The mechanical properties of the face sheets, and PVC foam cores (assumed isotropic) are provided in Table 1.

A specimen length, $L = 305$ mm was chosen; face sheet thickness, h_f, in the range 2–6 mm, and core thickness, $h_c = 25.4$ and 50.8 mm were examined. A unit load ($P/b = 1$ N/mm; unit width considered) was applied for several crack lengths, and root rotation angle (ϕ) was evaluated at the crack tip. For the foundation analysis, a minimum intact length portion, $L_{b,min} = L - a_{max}$ was maintained [18]. All analyses were carried out under plane stress conditions.

3. Results and discussions

3.1. Root rotation results

The root rotation angle (ϕ) was determined from the displacements of the face sheet at the crack root obtained from FEA. The analytical root rotation angle was obtained by substituting the coefficients c_M and c_V (Equations. 6) in (1). c_M and c_V results for the various sandwich specimens are listed in Tables 2 and 3. The results are based on angle in degrees, and moduli in N/mm^2 and thickness in mm.

The results for c_M and c_V listed in Tables 2 and 3 were used to calculate the root rotation angle according to Equation (1). Fig. 4 shows rotation angle obtained from FEA and Equation (6) plotted vs. normalized crack length (a/L) for the range of face sheets and cores considered. For an Al/H100 specimen with a core thickness, $h_c = 25.4$ mm, FEA and the analytical expression (Equations.(4) and (5)) match closely for all face sheet thicknesses, see Fig. 4. The rotation angle decreases with increased face sheet thickness ($h_c = 25.4$ mm). A thicker core ($h_c = 50.8$ mm) will slightly increase the root rotation angle, see Fig. 4. At longer crack lengths, the analytical formula yields slightly higher rotation angles than the FEA. The deviation between analytical and FEA, however, is below 7%.

The analysis was also carried out to examine the influence of core modulus on the root rotation. A sandwich with E-glass/epoxy face sheet with $h_f = 4$ mm was chosen, along with three PVC foam cores with varying density. Refer to Table 1 for elastic properties of the face sheet, and the core. Fig. 5 shows the rotation angle (ϕ) plotted against normalized crack length (a/L). The analytical and

Table 1
Elastic properties of face sheets and PVC foam cores [16,17].

Elastic Properties	Aluminum (6061-T6)	E-glass/epoxy DBLT-850 (0/45/90/-45)	PVC H45	PVC H100	PVC H250
Young's Modulus, $E[MPa]$	68900	16400	55	135	260
Shear Modulus, $G[MPa]$	26000	5800	15	35	97
Poisson's ratio, $\nu[-]$	0.33	0.306	0.4	0.4	0.4
Density, $\rho[kg/m^3]$	–	–	48	100	250

Table 2
Analytical values for c_M and c_V for Al/PVC core specimens.

h_f	Al/H45		Al/H100		Al/H250	
[mm]	c_M	c_V	c_M	c_V	c_M	c_V
$h_c = 25.4$ mm						
3.2	3689	9896	2975	6437	2502	4551
4.76	3340	8114	2694	5278	2265	3732
6.35	3108	7025	2507	4569	2108	3231
$h_c = 50.8$ mm						
3.2	4387	13995	3979	11514	2975	6437
4.76	3972	11475	3204	7464	2694	5278
6.35	3696	9935	2981	6462	2507	4569

Table 3
Analytical values for c_M and c_V for E-glass/PVC core sandwich specimens.

h_f	E-glass/H45		E-glass/H100		E-glass/H250	
[mm]	c_M	c_V	c_M	c_V	c_M	c_V
$h_c = 25.4$ mm						
2	2898	6107	2337	3972	1965	2809
4	2437	4318	1965	2809	1653	1986
6	2202	3526	1776	2293	1493	1622
$h_c = 50.8$ mm						
2	3446	8637	2779	5618	2337	3972
4	2898	6107	2337	3972	1965	2809
6	2619	4986	2112	3243	1776	2293

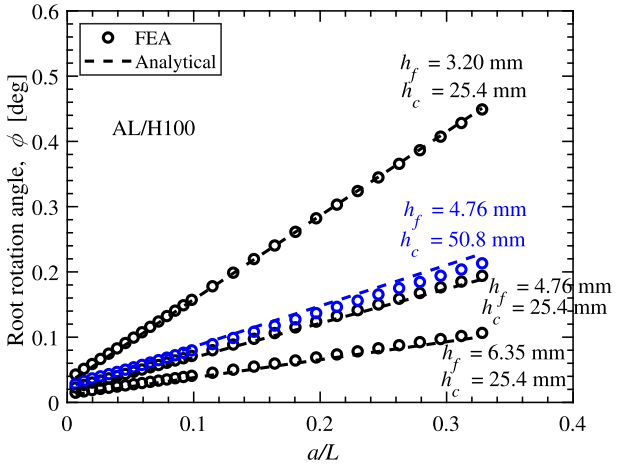

Fig. 4. Root rotation angle, ϕ vs. normalized crack length for Al/H100; h_f = 3.2, 4.76 and 6.35 mm; P = 1 N/mm.

FEA results for the softest core, H45, agree closely. With increased core modulus, and crack length, a/L, the rotation angle calculated by analytical expression exceeds the FEA results, but the results are quite close. The largest deviation (11.5%) was observed for the H250 core.

3.2. Energy-release rate and phase angle of SCB sandwich specimen

The compliance and energy-release rate of the SCB specimen is obtained from a foundation model [10,19,20]:

$$G = \frac{2P^2\lambda^2}{bk}\left[\lambda^2 a^2 + 2\lambda a + 1\right] \tag{7}$$

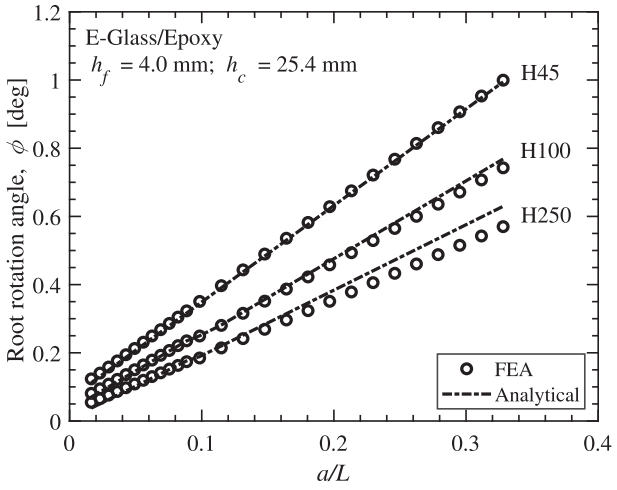

Fig. 5. Root rotation angle, ϕ vs. normalized crack length for E-glass epoxy and various PVC foam cores; h_f = 4 mm, h_c = 25.4 mm; P = 1 N/mm.

Based on dimensional considerations and beam theory analysis, the energy-release rate of a face sheet supported by a rigid foundation may be normalized by,

$$G_{BT} = \frac{6a^2(P/b)^2}{E_f h_f^3} \tag{8}$$

Sandwich specimen with aluminum face thicknesses, h_f = 3.20 mm and core thickness, h_c = 25.4 mm was considered. The bimaterial parameters, Σ, and, α, used by Li et al. [8] are defined as:

$$\Sigma = \bar{E}_f / \bar{E}_c \tag{9}$$

$$\alpha = (\Sigma - 1)/(\Sigma + 1) \tag{10}$$

The core modulus was chosen such that the sandwich system under consideration yielded Σ = 500 and α ∼ 1. A unit load P = 1 N/mm was applied, and G was recorded vs. crack length. Fig. 6a shows G vs. crack length (a/h_f). G increases strongly at short crack lengths due to the increased influence of shear force. The mode mixity phase angle (ψ) is shown vs. the normalized crack length in Fig. 6b. The predominant effect of shear is evident from the higher mode mixity phase angle at shorter crack lengths. The trends in both energy-release rate and mode-mixity phase angle qualitatively agree with the results for a delamination in elastic layers [8].

A set of sandwich specimens comprising of aluminum and E-glass face sheets thickness, h_f = 3.20, 4.76 and 6.35 mm and a range of core materials with thickness, h_c = 25.4 mm was considered. The core modulus was varied from 55 to 260 MPa. G was recorded at a crack length a/h_f = 5. Fig. 7 shows G/G_{BT} vs. modulus ratio, Σ (Equation (9)). The normalized energy-release rate increases with increasing Σ. The analytical G (see Equation (7)) with foundation modulus, $k = \bar{E}_c b/(h_c/4)$ agrees closely with the FEA results.

3.3. Compliance and crack length correction, Δ

A widely used method to determine the face/core interface toughness, G_c, is the modified beam theory (MBT) outlined in the ASTM draft standard [3] for SCB testing. This method refers to the

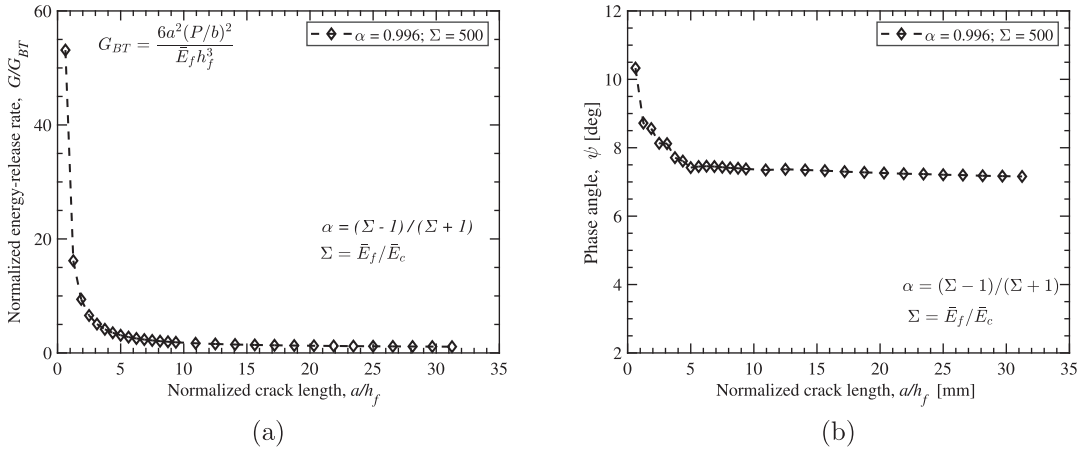

Fig. 6. (a) Energy-release rate vs. crack length (normalized) for SCB specimens with $\Sigma = 500$, (b) phase angle vs. normalized crack length (a/h_f) for an Al/H100 specimen with face sheet thicknesses, $h_f = 3.20$ and 6.35 mm and core thickness, $h_c = 25.4$ mm.

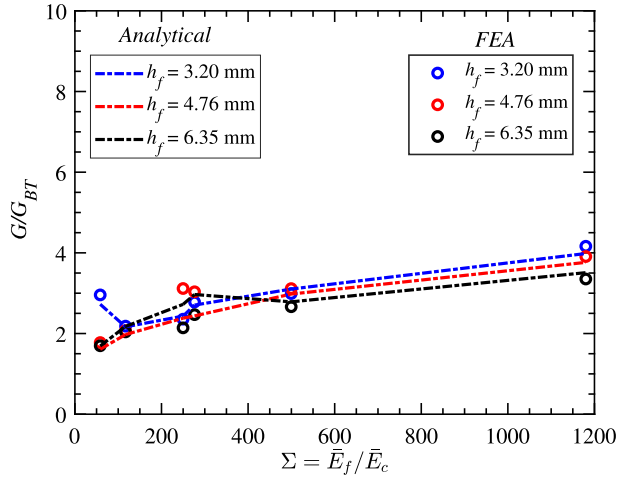

Fig. 7. Energy-release rate vs. $\Sigma = \bar{E}_f/\bar{E}_c$ for SCB specimens with $h_f = 3.20$, 4.76 and 6.35 mm and core thickness, $h_c = 25.4$ mm; ($a/h_f = 5$).

initiation of debond growth because it uses the load and displacement (P_c and δ_c) at the onset of debond growth. G_c is determined by:

$$G_c = \frac{3P_c\delta_c}{2b(a+\Delta)} \tag{11}$$

where b is the specimen width, and a is the crack length. Δ is the offset crack length, refer to Fig. 8a. With this correction, it is possible to express the compliance of the SCB specimen using classical beam theory,

$$C = \frac{1}{3\bar{E}_f I_f}(a+\Delta)^3 \tag{12}$$

Δ is determined from the experimental crack length, and compliance, C, data. By plotting the cube root of compliance vs. crack length as shown in Fig. 8b, it is possible to determine Δ by extrapolation to zero compliance. The offset crack length, Δ, may also be determined from the foundation model expression for the compliance, see Appendix B.

$$\Delta = h_f^{3/4}\sqrt[4]{\frac{\bar{E}_f h_c}{12E_c}} \tag{13}$$

4. Fracture testing of sandwich SCB specimen

4.1. Materials and method

Two sandwich systems were tested and evaluated against numerical and analytical models. The face sheet comprised of a 4-ply and 8-ply 5320–1/T650 plain weave (PW) Carbon Fiber Reinforced Plastic (CFRP) prepreg with a stacking sequence $[(\pm 45°)/(0°/90°)/(0°/90°)/(\pm 45°)]$ and $[(\pm 45°)/(0°/90°)/(0°/90°)/(\pm 45°)]$s, respectively (cured ply thickness (CPT) = 0.185 mm). Two types of Nomex® based honeycomb cores were employed, both with thickness of 12.7 mm. Thus, the two types of sandwich systems fabricated were (a) face sheet thickness, $h_f = 1.47$mm, core density = 96 kg/m^3, cell size = 3.2 mm, (b) face sheet thickness, $h_f = 0.74$mm, core density = 48 kg/m^3, cell size = 9.5 mm. The sandwich panels were vacuum bagged and cured in an autoclave under a pressure of 0.2 MPa. The SCB specimens (254 × 50.8 mm, pre-crack length = 50.8 mm) were cut from the panels after cure using a band saw cutter. The specimens were then air dried and piano hinges (length = 25.4 mm) were bonded to top face sheet using an epoxy-based adhesive.

In a sandwich Single Cantilever Beam (SCB) specimen, a vertical force is applied to the top face sheet with the bottom face sheet rigidly fixed, see Fig. 1. As the crack propagates, the fracture tests should remain in the mode I regime, the crack tip stress field must be devoid of any shear component. This can be achieved by enforcing the load application point to always remain vertical. Such an arrangement mandates either a long load application arm or let the specimen slide in the longitudinal direction. The latter option was chosen and a SCB test rig base on the translatable rig was fabricated at the National Institute for Aviation Research (NIAR) and is shown in Fig. 9. The slide and rail system comprised of low friction bearing to ensure smooth sliding of the specimen. The crack propagation was monitored with the aid of a digital microscope and ruler. The setup was installed on a 220 kip servo-hydraulic test machine, and the force and displacement of the loading were recorded at a frequency of 10 Hz until the test was stopped. Load was introduced at a constant displacement rate of 5 mm/min until the crack propagated an increment of about 50 mm, after which the specimen was unloaded.

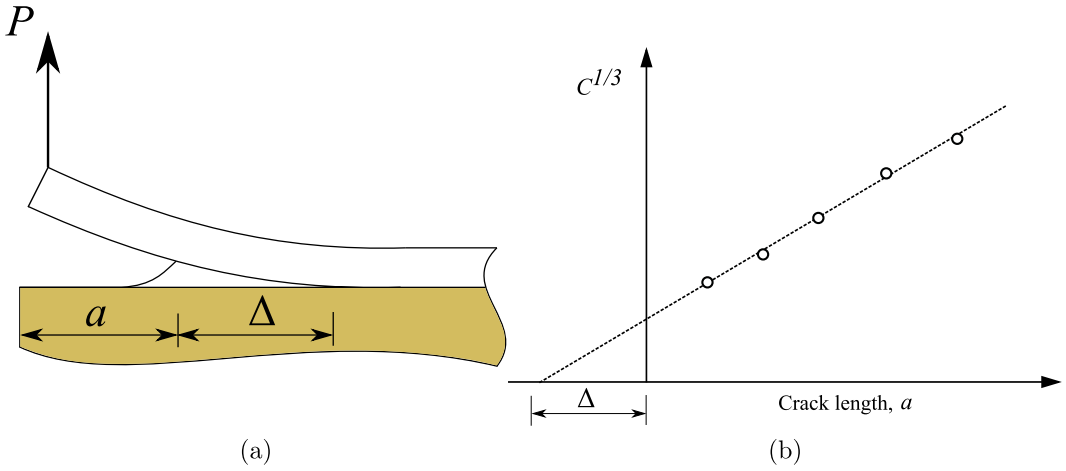

Fig. 8. (a) Crack length correction, Δ, and (b) determination of offset crack length, Δ, according to MBT.

4.2. Compliance of sandwich SCB specimen: comparison against the foundation model

In the SCB fracture tests, the core density, cell-size and face sheet thickness were varied across two configurations [21]. Seven specimens of each configuration were tested. The face sheet material properties were obtained from the National Center for Advanced Material Performances (NCAMP) directory at NIAR [22]. Moreover, the honeycomb core properties were obtained using the proposed closed-form expressions for a double cell wall configuration by Malek and Gibson [23]. The analytical model of Gibson requires the cell wall dimensions, cell wall paper properties and thickness as input, and have been proven to be robust in numerous Finite Element (FE) based models [15,24–26]. The material properties of honeycomb cores and face sheet are provided in Tables 4 and 5, respectively. In Table 4, note that each core type is distinguished using the notation: HRH10-cell size-density.

In order to compare the SCB specimen performance against the foundation based analytical model, the experimental compliance was obtained from the load arm displacement and load cell, $C = \delta/P$. The compliance from the FE-model was obtained directly from the load application node, see Fig. 3. Fig. 10 shows compliance vs crack length (normalized) for two sandwich configurations considered here. The FE-model closely follow the values predicted using the foundation model with the foundation modulus, $k = \overline{E}_c b/(h_c/4)$ (refer to Equation (3b)). For the thicker face sheet specimen (8-ply, $h_f = 1.47$ mm), experimentally obtained compliance values closely follow both foundation and FE-model at all crack lengths. For the case with largest cell size of 9.5 mm and thin face sheet (4-ply, $h_f = 0.74$ mm), both foundation and FE-models were found to

Table 4
Material properties of Nomex® HRH-10 cores deduced from Gibson-Ashby approach [23].

	HRH-10-3.2-96	HRH-10-9.5-48
E_L [Mpa]	2.9	0.2
E_W [Mpa]	2.9	0.2
E_T [Mpa]	414	117
ν_{LW}	0.99	0.99
ν_{TL}	0.03	0.0008
ν_{TW}	0.4	0.4
G_{LW} [Mpa]	0.13	0.01
G_{TL} [Mpa]	55	16
G_{TW} [Mpa]	88	25
Core Density [kg/m^3]	96	48
Cell size [mm]	3.2	9.5
Single cell wall thickness [μm]	125	196

Table 5
5320–1/T650 PW (plain-weave) face sheet material properties [22].

E_{11}	E_{22}	E_{33}	ν_{12}	ν_{13}	ν_{23}	G_{12}	G_{13}	G_{23}
[**MPa**]	[**MPa**]	[**MPa**]	[-]	[-]	[-]	[**MPa**]	[**MPa**]	[**MPa**]
67300	62500	10800	0.06	0.52	0.51	5650	3630	3830

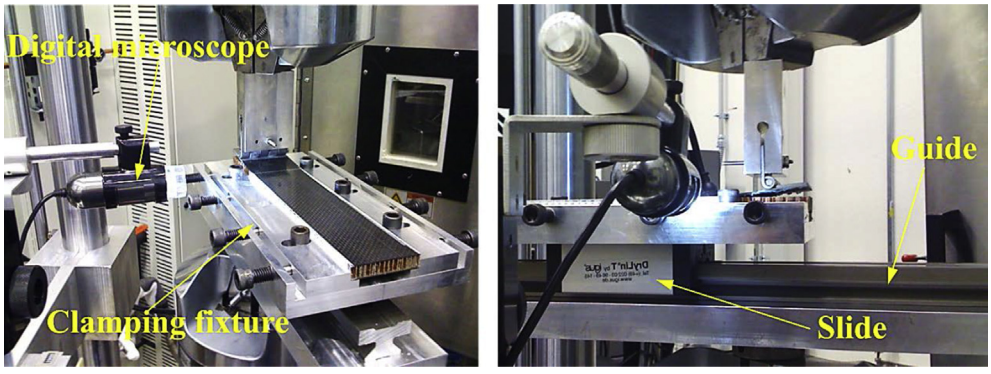

Fig. 9. A translatable base SCB test fixture fabricated at NIAR [21].

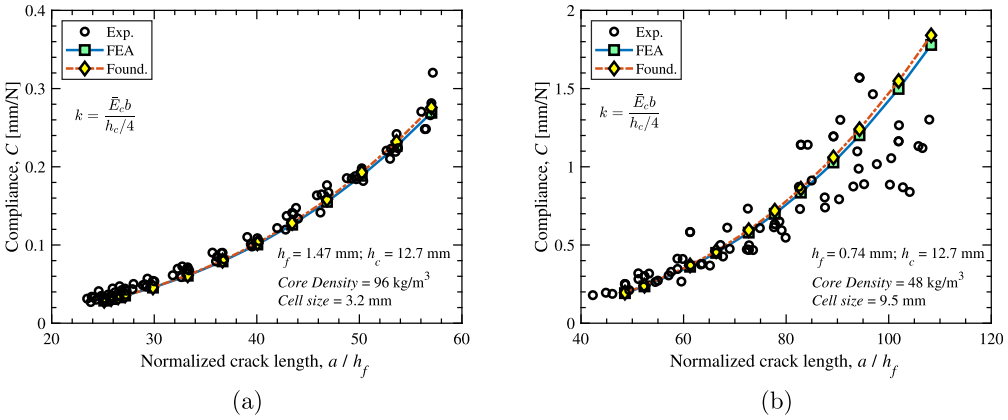

Fig. 10. Compliance vs. normalized crack length (a/h_f) for 5320–1/T650 PW/Nomex® HRH-10 honeycomb core sandwich SCB specimens.

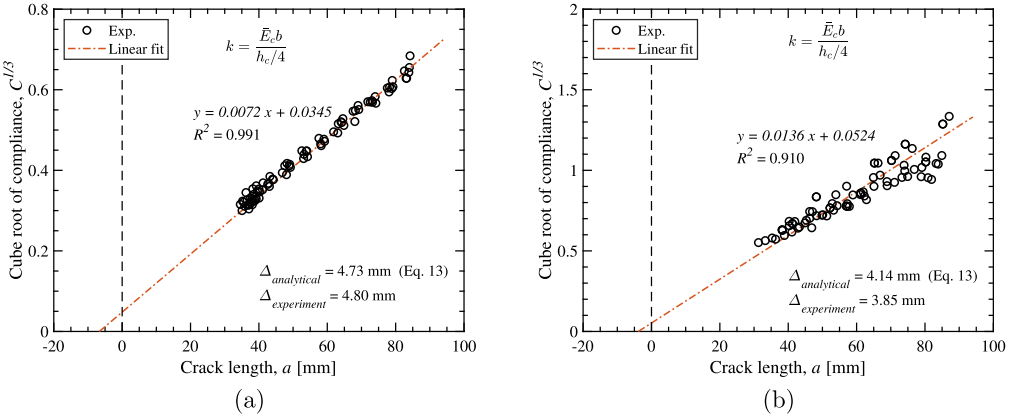

Fig. 11. Compliance$^{1/3}$ vs. crack length for 5320–1/T650 PW/Nomex® HRH-10 honeycomb core (h_c = 12.7 mm) sandwich SCB specimens (a) h_f = 1.47 mm, core density = 96 kg/m^3, cell size = 3.2 mm, (b) h_f = 0.74 mm, core density = 48 kg/m^3, cell size = 9.5 mm.

closely match with the experimentally obtained compliance at shorter crack lengths, see Fig. 10. The specimens with larger cell size showcased abrupt debonding, which might have led to the scatter for crack lengths $a/h_f > 85$, see Fig. 10b. This may also be attributed to discontinuous crack growth due to the large cells.

Compliance$^{1/3}$ vs. crack length plots for the two sandwich systems under consideration is shown in Fig. 11. The offset crack lengths, Δ, calculated using Equation (13) for both specimens are provided in the inset. For the specimen with thick face sheet (8-ply), Δ, obtained using the foundation model expression (Equation (13)) agrees very well (within 1.5%) with experimentally calculated crack offset length. Whereas, for the specimen with thinner face sheet (4 ply), Equation (13) slightly over-predicts the experimentally obtained offset crack length by 7%. This deviation may be attributed to the scatter in compliance data, especially at larger crack lengths due to large cell size, see Fig. 11b.

5. Conclusions

Closed-form expressions for the crack root rotation angle for a SCB sandwich fracture specimen were derived based on an elastic foundation model. The obtained expressions include the moduli and thicknesses of the face sheet, and core. Finite element analyses showed close agreement with the analytical results. For the range of sandwich specimens chosen in this study, the energy-release rate expression derived from the foundation model agreed well with FEA predictions. Moreover, from the FE analysis it was shown that the energy-release rate and mode mixity phase angle increase with decreasing crack length which is due to the effect of transverse shear. Equivalency of compliance expressions obtained using elastic foundation model, and built-in beam approach was considered to derive an analytic estimate of crack length correction factor, Δ. The offset crack length increases with increased face sheet thickness and modulus, and decreases with increased core modulus. In addition, the Winkler based foundation model with the proposed foundation modulus correlating quarter thickness of the core was evaluated against fracture tests. The experimentally obtained compliance for SCB specimens with two face thicknesses and two types of cores were found to closely match with both analytical and numerical predictions.

Conflicts of interest

The authors declare that there is no conflicts of interest.

Acknowledgements

The financial support from the EUDP (Grant: 6410-0602) for the DTU part of this research is gratefully acknowledged. The second author's research has been supported by grants from FAA, NIA and ONR. The FAA, NIA and ONR program managers, Dr. Larry Ilcewicz, Dr. Zhi Chen, Dr. Ronald Krueger and Dr. Yapa Rajapakse showed keen interest in this project and are gratefully acknowledged.

Appendix A. CSDE Method

A highly refined crack tip mesh is utilized for the CSDE method, refer to Fig. 3. The relative crack flank displacements (δ_x and δ_y) are employed to compute the energy-release rate Hutchinson and Suo [14]:

$$G = \frac{\pi\left(\delta_x^2 + \delta_y^2\right)}{2x(c_1 + c_2)} \tag{A.1}$$

δ_x refers to the relative sliding displacement, δ_y to the opening displacement, and x is the distance behind the crack tip. The stiffness parameters, c_m, are given by:

$$c_m = \frac{\kappa_m + 1}{G_m} \tag{A.2}$$

where $m = 1$ and 2 for face sheet, and core, respectively. G_m is the shear modulus. $\kappa_m = 3 - 4\nu_m$ for plane strain, and $\kappa_m = (3 - 4\nu_m)/(1 + \nu_m)$ for plane stress conditions where ν_m is the Poisson's ratio. The mode mixity phase angle is expressed as:

$$\psi = \tan^{-1}\left(\frac{\delta_x}{\delta_y}\right) \tag{A.3}$$

The mode-mixity phase angle is referred to as the "reduced" formulation. In the CSDE method, G and ψ are calculated at various locations behind the crack tip. The results at the crack tip are obtained by extrapolation to $x = 0$. For more details, refer to Ref. [13,27]. A standard FE code can be utilized to extract the displacements. Here, the CSDE method was implemented as a separate subroutine in ANSYS®.

Appendix B. Calculation of crack length offset

The foundation model and beam-theory expressions for the SCB sandwich specimen compliance are:

$$C_{EFM} = \frac{4\lambda}{k}\left[\frac{\lambda^3 a^3}{3} + \lambda^2 a^2 + \lambda a + \frac{1}{2}\right] \tag{B.1}$$

$$C_{BT} = \frac{1}{3\overline{E}_f I_f}(a + \Delta)^3 \tag{B.2}$$

Calculation of Δ is formally done by equating the two compliance expressions, but is obstructed by the 3rd order expressions. If the beam-theory expression (Equation B.2) is expanded, we will obtain:

$$C_{BT} = \frac{1}{3\overline{E}_f I_f}\left(a^3 + 3a^2\Delta + 3a\Delta^2 + \Delta^3\right) \tag{B.3}$$

Matching terms with equal power in crack length leads to:

$$a^3 : \frac{4\lambda^4}{3k} = \frac{1}{3\overline{E}_f I_f} \tag{B.4a}$$

$$a^2 : \frac{4\lambda^3}{k} = \frac{\Delta}{\overline{E}_f I_f} \tag{B.4b}$$

$$a : \frac{4\lambda^2}{k} = \frac{\Delta^2}{\overline{E}_f I_f} \tag{B.4c}$$

$$a^0 : \frac{2\lambda}{k} = \frac{\Delta^3}{3\overline{E}_f I_f} \tag{B.4d}$$

The first Equation B.4a does not provide Δ, but is satisfied exactly, while the remaining equations yield the following expressions for Δ:

$$\Delta_2 = \frac{4\lambda^3 \overline{E}_f I_f}{k} \tag{B.5a}$$

$$\Delta_1 = 2\lambda\sqrt{\frac{\overline{E}_f I_f}{k}} \tag{B.5b}$$

$$\Delta_0 = \sqrt[3]{\frac{6\lambda\overline{E}_f I_f}{k}} \tag{B.5c}$$

where the subscript on Δ indicate the power of crack length. It can be easily verified that $\Delta_2 = \Delta_1$.

These results will be illustrated for a set of sandwich specimens with aluminum face sheets of 2, 4 and 6.35 mm thickness with 25.4 mm thick H45, H100 and H250 PVC foam cores. The material properties of the face sheets, and PVC cores are provided earlier (Table 1). Results for Δ_1, Δ_2 and Δ_3 along with the "exact" value obtained by numerically solving Equation B.1 at crack lengths of 25, 35 and 45 mm are summarized in Table B.1.

Table B.1
Estimate of Δ for selected SCB sandwich specimens.

Core	h_f [mm]	$\Delta_1 = \Delta_2$ [mm]	Δ_0 [mm]	Δ (exact) [mm]
H100	6.35	23.15	26.5	23.67 ± 0.07
	4.0	16.37	18.74	16.60 ± 0.41
	2.0	9.73	11.14	9.79 ± 0.01
H45	6.35	28.71	32.86	29.54 ± 0.10
H250	6.35	19.47	22.28	19.82 ± 0.06

It is noted that all the estimates of Δ agree reasonably with the exact value and that Δ_1 is very close to the exact value. It is therefore, recommended to use Δ_1 for estimation of the crack length offset,

$$\Delta = 2\lambda\sqrt{\frac{\overline{E}_f I_f}{k}} \tag{B.6}$$

Upon substitution of foundation modulus expression, k, from Equation (3b), Δ can be expressed in terms of face sheet and core material and geometrical parameters as:

$$\Delta = h_f^{3/4}\sqrt[4]{\frac{\overline{E}_f h_c}{12E_c}} \tag{B.7}$$

References

[1] R. Fields, R. Zarda, Analysis and Test Methodology for Fracture Mechanics of Unbonded Sandwich Structures, Martin Maerietta Task Report, EDF No. MM0 TKR 10722739-001, 1994.

[2] W.J. Cantwell, P. Davies, A study of skin-core adhesion in glass fibre reinforced sandwich materials, Appl. Compos. Mater. 3 (1996) 407–420.
[3] ASTM Draft Standard, Mode I Dominant Facesheet-To-Core Fracture Toughness of Sandwich Constructions (ASTM WK56166), Technical Report, American Society for Testing and Materials, West Conshohocken, PA, 2018.
[4] K. Shivakumar, H. Chen, S.A. Smith, An evaluation of data reduction methods for opening mode fracture toughness of sandwich panels, J. Sandw. Struct. Mater. 7 (2005) 77–90.
[5] M.F. Kanninen, An augmented double cantilever beam model for studying crack propagation and arrest, Int. J. Fract. 9 (1973) 83–92.
[6] J. Williams, Large displacement and end block effects in the 'DCB' interlaminar test in modes I and II, J. Compos. Mater. 21 (1987) 330–347.
[7] J. Williams, End corrections for orthotropic DCB specimens, Compos. Sci. Technol. 35 (1989) 367–376.
[8] S. Li, J. Wang, M. Thouless, The effects of shear on delamination in layered materials, J. Mech. Phys. Solid. 52 (2004) 193–214.
[9] M.G. Andrews, R. Massabò, The effects of shear and near tip deformations on energy release rate and mode mixity of edge-cracked orthotropic layers, Eng. Fract. Mech. 74 (2007) 2700–2720.
[10] V. Saseendran, L.A. Carlsson, C. Berggreen, Shear and foundation effects on crack root rotation and mode-mixity in moment- and force-loaded single cantilever beam sandwich specimen, J. Compos. Mater. 52 (2018) 2537–2547.
[11] G.A. Kardomateas, Z. Yuan, L.A. Carlsson, Elastic foundation constants for sandwich composites, AIAA J. 56 (2018) 4169–4179.
[12] ANSYS Inc, ANSYS® Mechanical User's Guide, 2015.
[13] C. Berggreen, B.C. Simonsen, K.K. Borum, Experimental and numerical study of interface crack propagation in foam-cored sandwich beams, J. Compos. Mater. 41 (2006) 493–520.
[14] J. Hutchinson, Z. Suo, Mixed mode cracking in layered materials, Adv. Appl. Mech. 29 (1991) 63–191.
[15] V. Saseendran, P. Varatharaj, S. Perera, W. Seneviratne, Damage initiation and fracture analysis of honeycomb core single cantilever beam sandwich specimens, J. Sandw. Struct. Mater. (2020), https://doi.org/10.1177/1099636220909820.
[16] Diab Group, Divinycell H Technical Data, 2016.
[17] M. Manca, A. Quispitupa, C. Berggreen, L.A. Carlsson, Face/core debond fatigue crack growth characterization using the sandwich mixed mode bending specimen, Compos. Appl. Sci. Manuf. 43 (2012) 2120–2127.
[18] X. Li, L.A. Carlsson, Elastic foundation analysis of tilted sandwich debond (TSD) specimen, J. Sandw. Struct. Mater. 2 (2000) 3–32.
[19] X. Li, L.A. Carlsson, The tilted sandwich debond (TSD) specimen for face/core interface fracture characterization, J. Sandw. Struct. Mater. 1 (1999) 60–75.
[20] J.G. Ratcliffe, J.R. Reeder, Sizing a single cantilever beam specimen for characterizing facesheet-core debonding in sandwich structure, J. Compos. Mater. 45 (2011) 2669–2684.
[21] J.S. Tomblin, W. Seneviratne, S. Denning, Mode I (G1c) Fracture Toughness of Composite Sandwich Structures for Use in Damage Tolerance Design and Analysis : Vol . I Static Testing Including Effects of Fluid Ingression, Technical Report, Federal Aviation Adminstration, New Jersey, 2017. DOT/FAA/TC-16/23.
[22] E. Clarkson, Cytec Cycom 5320-1 T650 3k-PW Fabric Material Allowables Statistical Analysis Report, NCP-RP-2012-023 Rev NC, Technical Report, National Institure for Aviation Research (NIAR), Wichita State University, 2015.
[23] S. Malek, L. Gibson, Effective elastic properties of periodic hexagonal honeycombs, Mech. Mater. 91 (2015) 226–240.
[24] V. Saseendran, C. Berggreen, Mixed-mode fracture evaluation of aerospace grade honeycomb core sandwich specimens using the double cantilever beam–uneven bending moment test method, J. Sandw. Struct. Mater. 22 (2020) 991–1018.
[25] M. Tauhiduzzaman, L.A. Carlsson, Influence of constraints on the effective inplane extensional properties of honeycomb core, Compos. Struct. 209 (2019) 616–624.
[26] V. Saseendran, Fracture Characterization and Analysis of Debonded Sandwich Composites, Ph.D. Thesis, Department of Mechanical Engineering, Technical University of Denmark (DTU), 2017.
[27] V. Saseendran, C. Berggreen, R. Krueger, Mode mixity analysis of face/core debonds in a single cantilever beam sandwich specimen, J. Sandw. Struct. Mater. (2018), https://doi.org/10.1177/1099636218788223.